ELSEVIER

Tectonophysics 259 (1996) 67–80

TECTONOPHYSICS

Paleoseismicity studies on the Oca–Ancón fault system, northwestern Venezuela

Franck A. Audemard M.

Venezuelan Foundation for Seismological Research (FUNVISIS) Apartado Postal 76880, Caracas 1070-A, Venezuela

Received 11 November 1994; accepted 4 October 1995

Abstract

The E–W-trending, right-lateral Oca–Ancón fault system extends eastward for 650 km, from the Colombian Caribbean coast near the city of Santa Marta to the town of Boca de Aroa (located on the eastern coast of Falcón State, northwestern Venezuela), across the Goajira peninsula, the outlet of Lake Maracaibo, the coastal plains of Buchivacoa and the central Falcón range. This system is very conspicuous west of the city of Maracaibo where its single trace sharply truncates the northern ends of the Santa Marta block and the Perijá range.

Fault-related landforms along the system trace (e.g., displaced beach strandlines at Sinamaica and fault scarplets in the Buchivacoa plains) suggest that it may have been active during Holocene times. A first trenching attempt carried out north of Maracaibo (at Sinamaica) in 1969 only confirmed its Holocene tectonic activity.

On the western coastal plains of Falcón State and east of Lake Maracaibo, the system is less simple as it is composed of two parallel fault strands but they are clearly evidenced by Holocene paleoseismic scarplets. Recently, this system has been paleoseismically evaluated by means of two trenches placed across each of the two parallel branches known as the Oca and the Ancón faults. Dimensions of these bulldozer-dug trenches are 80 m long and 8 m deep.

Various lines of evidence obtained from these exploratory trenches indicate that: (a) three surface rupture events, dated slightly prior to 7755 ± 320, 6240 ± 39‸ and 1945 ± 630 yr B.P., have occurred along the Oca fault; (b) one surface rupture event has occurred within the past 3125 ± 185 yr on the Ancón fault; (c) the Holocene slip rate of the system is close to 2 mm/yr; and (d) either of the faults can generate a maximum event of magnitude 7.4–7.5. Recurrence of such earthquakes on the Ancón fault is close to 1900 years while it is about 4300 years on the Oca fault.

1. Introduction

The Oca–Ancón fault system is a major E–W-trending, right-lateral strike-slip tectonic feature of northern South America which trace extends eastward from the Colombian village of Santa Marta to the town of Boca de Aroa, located on the eastern coast of Falcón state (northwestern Venezuela). This fault system crosses the Goajira peninsula, the outlet of lake Maracaibo, the coastal plains of Buchivacoa (northwestern Falcón State) and the central Falcón range and it sharply truncates the northern ends of the Santa Marta block (northern Colombia) and Perijá range (its summits constitute the Colombian–Venezuelan border). The Oca–Ancón system converges with the Boconó–San Sebastián–El Pilar system, considered by many workers as the major southern boundary of the Caribbean plate, on the Aroa–Golfo Triste depression (Fig. 1).

Spectacular diagnostic geomorphic features of Quaternary activity have been reported along this tectonic system since the late forties. Voorwijk (1948)

SSDI 0040-1951(95)00144-1

photo-interpreted several kilometers long fault scarplets related to both Oca and Ancón faults in the Quaternary alluvial plains of Buchivacoa, some 50 km east of Maracaibo. Few years later, Miller (1960) observed the displacement of Holocene beach strandlines in Sinamaica, slightly north of the city of Maracaibo. This second site was trenched by Cluff and Hansen (1969) who could put in evidence the Holocene activity of the Oca fault but they could only establish the occurrence of the latest seismic event on that segment of the system which has happened within the last 2700 years.

Despite all these evidences, many authors in recent times have seismically underestimated this fault system (Schubert and Sifontes, 1970; Dewey, 1972; Kafka and Weidner, 1981; Cisternas and Gaulon, 1984; Stephan, 1985; Morris et al., 1990) and some of them have considered it inactive. On the contrary, other authors have overestimated its lateral displacement to fit Caribbean geodynamics models. In fact, along the axis of the Falcón anticlinorium, Oligocene outcrops on both sides of the fault system lead to estimates of apparent dextral displacement of 30 ± 3 km (Soulas et al., 1987; Audemard, 1991). Moreover, Janssen (1979) has proposed no more than 50 km of post-middle Cretaceous apparent right-lateral displacement along this system based on the apparent offset of the Cogollo Group isopach map from northern Lake Maracaibo and Tschanz et al. (1974) have estimated 65 km of apparent right-lateral offset measured on Mesozoic metamorphic rocks. These estimates do not fit in many geodynamics models where large transcurrent movements are required along the southern boundary of the Caribbean plate.

Very few authors have mapped thoroughly the fault trace farther east of Maracaibo since the fifties (Jaeckli and Erdman, 1952; Mendez and Guevara, 1969; Soulas et al., 1987; Audemard, 1991; Audemard et al., 1992) where profuse geophysical and geological information has been collected by oil companies for decades. In fact, this fault system has very frequently been sketched across the Falcón anticlinorium without any field corroboration (Bellizzia et al., 1972; Malfait and Dinkelman, 1972; Vasquez and Dickey, 1972; Kellogg and Bonini, 1982; Stephan, 1982; Cabrera de Molina, 1982, 1985; Schubert and Krause, 1984; Gallardo, 1985; Pindell et al., 1988), following diverse positions and trends

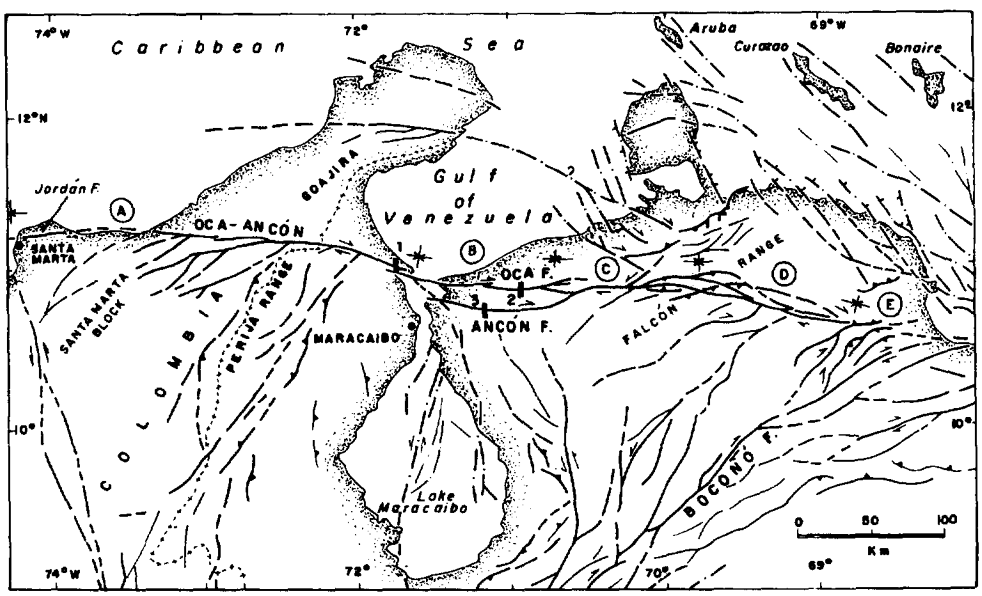

Fig. 1. Neotectonic map of northwestern Venezuela and northern Colombia. The most relevant tectonic feature of the region is the E–W-trending right-lateral strike-slip Oca–Ancón fault system. Capital letters identify fault segments and small boxes identify trench sites: *1*—Cluff and Hansen (1969), *2* and *3*—Audemard (1991). Map sources: Miller (1960), Tschanz et al. (1969), Kellogg and Bonini (1982), Soulas (1985), Soulas et al. (1987), Audemard (1991) and Audemard et al. (1992).

in order to connect the well-known western segment of the fault (west of Maracaibo) with the Boconó–San Sebastián–El Pilar fault system (Audemard, 1993).

2. Active trace of the Oca–Ancón fault system

The detailed mapping of the active trace of the Oca–Ancón fault system allows to subdivide it into five different segments (Fig. 1), from west to east:

(A) Between the city of Santa Marta and the outlet of lake Maracaibo (Toas island). This segment is the simplest among the others as it is composed of a main trace that truncates the northern termination of the Perijá range (known as Montes de Oca from where the name of the fault derives). Westward it seems to control the linear northern coast of the Santa Marta block (Sierra Nevada de Santa Marta) where some potentially active minor faults, which are located south of the fault and NE–SW striking, converge with the main trace in a kind of horse tail structure; farther west it seems to connect with the E–W-striking Jordán fault, mapped east of Santa Marta.

(B) Between Toas island and the village of Mene de Mauroa. The fault trace of the system in this segment divides into two sub-parallel strands: the E–W-striking Oca and Ancón faults. Both traces are defined by several kilometers long fault scarplets in Quaternary alluvial terraces that were photo-interpreted by Voorwijk (1948). These faults limit a large area of probable recent subsidence which Audemard (1991, 1993) interpreted as an active pull-apart basin.

(C) Between the villages of Mene de Mauroa and Paraiso. The fault trace is very complex as several anastomosing strands converge on or diverge from the main lineament. The eastern portion of this fault segment, between the villages of Camare and Paraiso in central Falcón State, has been interpreted by Jaeckli and Erdman (1952), Audemard (1991) and Audemard et al. (1992) as a flower structure since the inner deformation in the fault zone is of strike-slip type while the outer deformation is characterized by reverse faults affecting Quaternary alluvial ramps rooted in both flanks of the Camare–Paraiso range.

All the above-mentioned segments strike roughly N090 to N100° (east–west).

(D) Between the village of Paraiso and the Aroa valley. This segment of the fault system is composed of several sub-parallel fault strands of relative short length in comparison with other segments of this major tectonic feature (Mendez and Guevara, 1969; Soulas et al., 1987; Audemard et al., 1992). This section of the Oca–Ancón system is WNW–ESE striking. The fault strands cut across the towns of Churuguara and Maparari and they run slightly oblique to the Tocuyo river course, until becoming tangent to it. The seismic activity near Churuguara in central Falcón State, which is characterized by small to moderate but persistent earthquakes, can be clearly associated to this WNW–ESE-trending segment of the Oca–Ancón fault system (Soulas et al., 1987; Audemard et al., 1992; Malave, 1992). The relatively high frequency of such small to moderate earthquakes could be imputed to the number and short length of the fault strands that compose the system in that region (Audemard and Romero, 1993).

(E) Between the villages of Socremo and Boca de Aroa. The fault system regains its original direction along the northern margin of the Aroa valley: aproximately east–west. The fault in this segment shows geomorphic features of reverse faulting where Quaternary alluvial ramps are tilted and flexed (Audemard et al., 1992).

3. Geological setting

In the western coastal plains of Falcón State and east of Maracaibo, the Oca–Ancón fault system is fairly simple as it is composed of two sub-parallel fault strands (segment B): the Oca and Ancón faults (Fig. 1). Their traces are defined by 10–15 km long scarplets in Quaternary alluvial ramps that were reported by Voorwijk (1948). Those scarplets face each other and they limit a large area of probable contemporary subsidence because large swamps are present, rivers become meandering and drainage flow is erratic (Graf, 1972). The western portion of this area is an active pull-apart basin located in the right-stepover between the dextral Oca and Ancón faults and related to the local transtension associated to the western end of the Ancón fault (Audemard, 1991, 1993).

This segment of the system was chosen for trenching among others because of technical facilities and favorable geological conditions, and mainly because the simplest segment of the system, the one west of Maracaibo, had already been trenched in the most favorable site [1 in Fig. 1; site described by Miller (1960) and excavated by Cluff and Hansen (1969)] which proved to be poorly satisfactory as trench excavation could not go beyond 2.5 m in depth due to shallowness of water table and unconsolidation of loose sands of Holocene beach strandlines. In consequence, two trenches were excavated (a trench per fault strand) in order to assess the seismic potential of this system (2 and 3 in Fig. 1).

4. Trench description and observations

Both trench sites were located on fault scarplets previously mentioned (2 and 3 in Fig. 1) and trenches were excavated by bulldozer down to 7 or 8 m in depth. They were cut perpendicular to the scarplet strike. Width of trenches decreased from 8 m at the top to 4 m at the bottom in order to stabilize trench walls and length varied between 80 and 85 m. Thus, removal of some 2500 to 3000 m^3 of material per trench was required.

5. The Hato El Guayabal trench on the Oca fault

This trench site, originally chosen by Soulas et al. (1987), is located on a 0.3 m high scarplet of the Oca fault, east of Casigua and near the village of Masuid (western Falcón State). This geomorphic feature was initially reported by Voorwijk (1948) from aerial photo-interpretation and its southward exposure, opposed to the gentle plain slope, was inferred by Fichter (1949) from presence of water accumulation and differential vegetation growth.

Geological observations made in trench walls (Fig. 2) allow us to put forward the following preliminary conclusions that have been considered in the paleoseismic interpretation proposed herein:

(1) The sedimentary sequence is mainly clayey but some silty-sand layers are interbedded with it. This few horizons represent higher energy levels of deposition whereas the clayey ones reflect periods of more quiet deposition that allow the development of brownish organic soils. On top of the sequence, a brown organic soil is forming nowadays.

(2) Right beneath the fault scarplet, deformation in trench wall corresponds to a smooth bend (great radius of bending) cut in the middle by a narrow, crevasse-shaped fault zone. the fault scarp is subdued and it has slightly retreated northward as scarplet faces (southward) against the gentle natural slope of this coastal plains.

(3) The persistence of surficial water circulation on the downthrown block is evidenced by the exclusive presence of channels within the sedimentary sequence of that block. This still occurs since a tiny channel flows on top of this fault compartment and runs parallel to the scarplet. Moreover, this micro-relief is responsible for water accumulation during the rainy season.

(4) The crevasse-shaped fault zone is filled by a brown, organic-rich material that could likely be composed by reworked paleosols related to scarp degradation. Fault planes on both sides of the crevasse strike between N080 and N100° and their dip varies between 55 and 90°N. Slickensides on the fault planes have a pitch varying between 15 and 45°W but the most frequent value is around 30°W. Striation features (tectoglyphs) establish that movement along the Oca fault is dextral with a relevant north-side-up reverse component. This microtectonic observation agrees very well with the bending observed in trench walls, the contemporary topography and the scarp morphology. Besides, this vertical component of movement along the Oca fault coincides with observations obtained from seismic profiles from segment B (Audemard, 1991, 1993).

(5) Deformation observed in trench walls is accommodated in both ductile and brittle manner. A 0.4 m throw can be estimated by using the thickest and lowermost silty-sand bed as reference. Besides, the whole interbedded sequence is slightly dragged on both blocks next to the fault plane. Thus, part of deformation is ductile due to the large clay content of the sequence. Due to bending, vertical throw measured on the youngest sandy marker is close to 0.90 m.

(6) ^{14}C dating has confirmed the Holocene age of the whole sedimentary sequence trenched at the Hato El Guayabal (Fig. 3). In Fig. 3, we can observe that ages of all markers of the footwall block are systematically older than their hanging-wall block equivalents. This fact might reflect a faster burial of or-

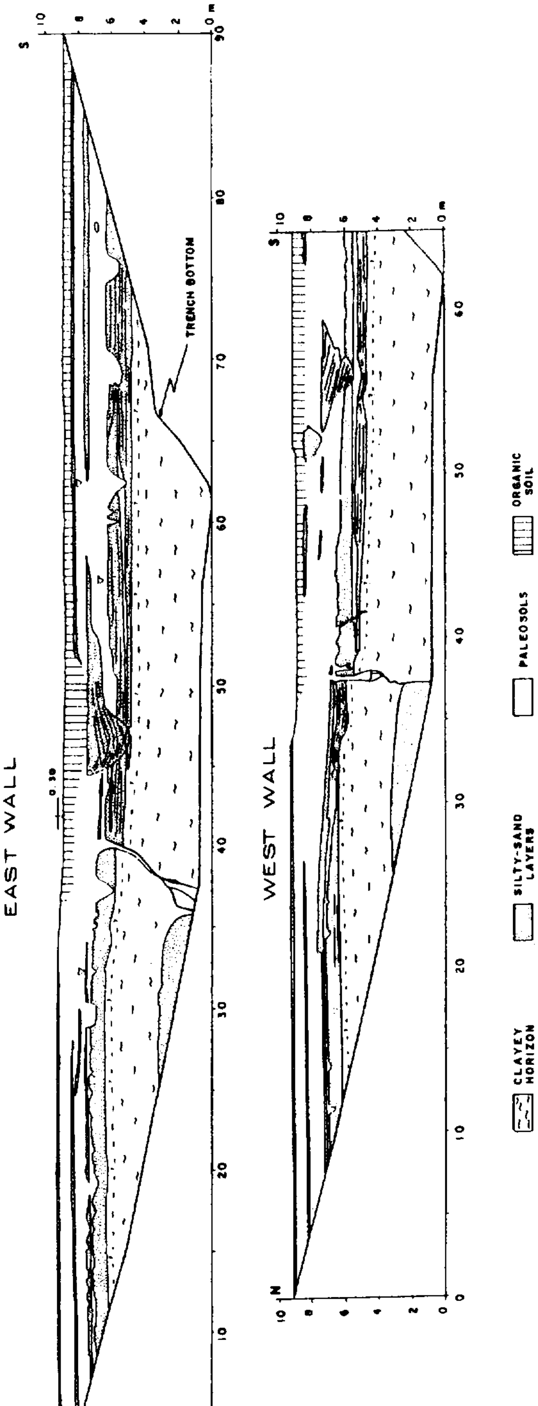

Fig. 2. Log of the Hato–El Guayabal trench across the Oca fault.

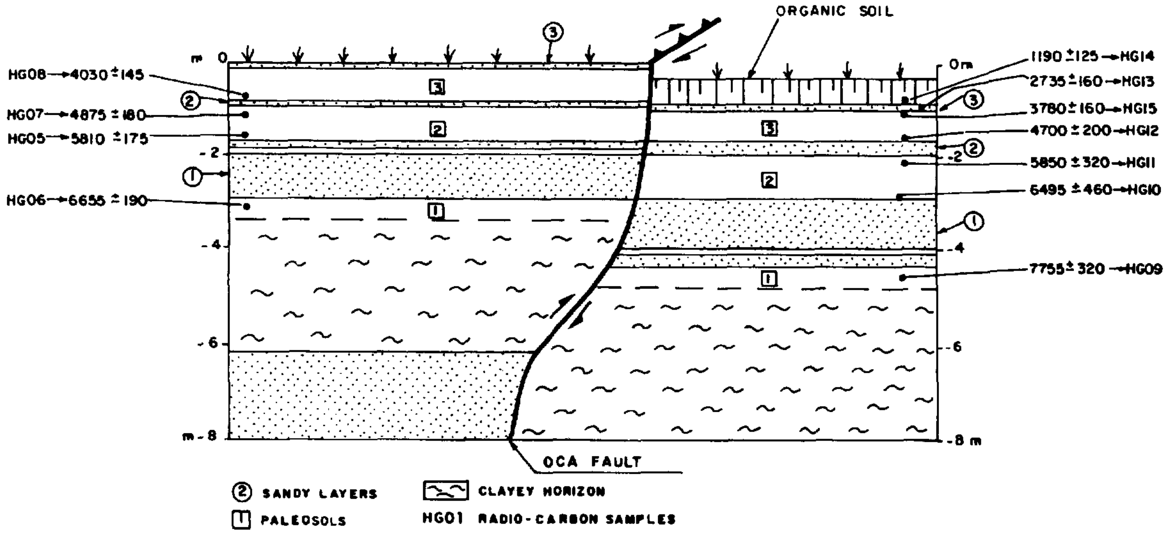

Fig. 3. Sampling locations and ^{14}C dating results of Holocene stratigraphic markers at the Hato–El Guayabal trench. Ductile deformation observed in trench walls is not represented.

ganic matter in the downthrown block and to a shorter time of aerial exposure, inhibiting rejuvenation of the dates. Therefore, we have considered that dating of markers belonging to the footwall block to be more representative of their true ages.

(7) Sedimentation near the fault is syntectonic as sandy beds are thicker in the southern downthrown block. Besides, as mentioned above, channels have always been restricted to this same block and contemporary organic soil is only developing on top of it as well.

For paleoseismic reconstruction purposes, the previous considerations oblige us to keep in mind that sedimentation near the fault has always been fundamentally related to and controlled by the fault activity (syn-sedimentary faulting). At first glance, we could be inclined to interpret that deformation observed in trench walls (both brittle and ductile) occurred during a single earthquake. Nevertheless, how could we explain the difference in thickness of the different sandy markers and the persistence of channels within the upper part of the Holocene sedimentary sequence of the downthrown block if a scarp did not exist during sedimentation?

These considerations have allowed us to propose a history involving the latest earthquakes occurred along the Oca fault that have controlled the sedimentation process. Aiming to a more realistic reconstruction, various attempts were done considering different possible scenarios: whole deformation accommodated in a fragile manner; whole deformation accommodated ductilely; various combinations of ductile and fragile deformation in different proportions and following different chronology paths. The reconstruction presented next seems to match better with the trench observations and it can explain very well the strong influence of active tectonics on sedimentation.

6. Paleoseismic interpretation of the Hato–El Guayabal trench

Trench geological observations combined with radiocarbon dates of several samples collected from selected stratigraphic horizons outcropping in the Hato–El Guayabal trench allowed us to make a paleoseismic reconstruction of the Oca–fault activity

Fig. 4. Paleoseismic reconstruction of the three latest earthquakes occurred on the Oca fault based on the data collected at the Hato–El Guayabal trench.

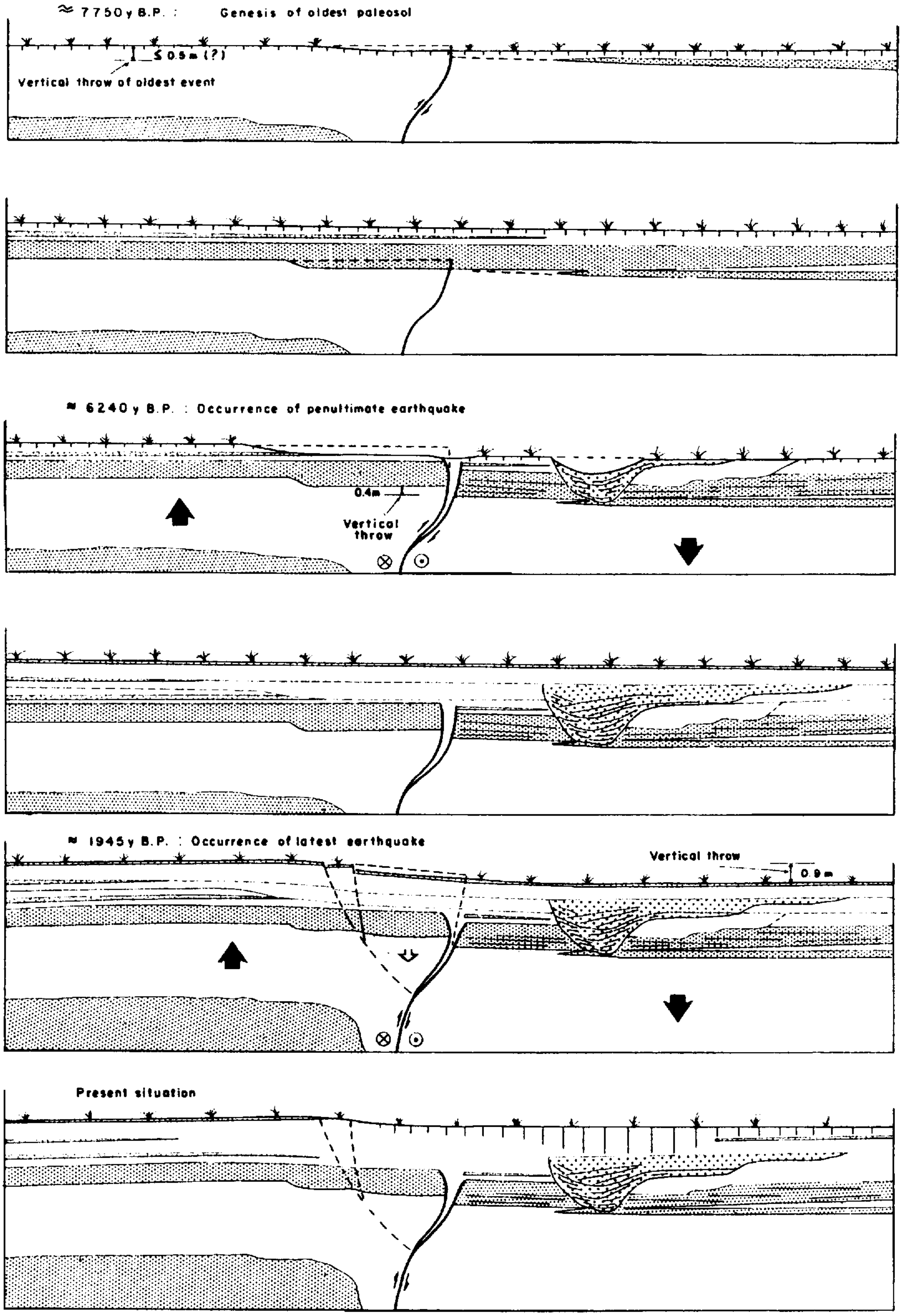
≈ 7750 y B.P. : Genesis of oldest paleosol
≲ 0.5 m (?)
Vertical throw of oldest event
≈ 6240 y B.P. : Occurrence of penultimate earthquake
0.4m
Vertical throw
≈ 1945 y B.P. : Occurrence of latest earthquake
Vertical throw
0.9 m
Present situation

Table 1
Results of the Oca fault paleoseismic evaluation at the Hato–El Guayabal trench

Occurrence (yr B.P.)	Vertical throw (m)	Vertical rate (mm/yr)	Total displacement (m)	Rate of displacement (mm/yr)	Magnitude (M_s)	Time elapsed inter-events (yr)
1945 ± 630	0.9	0.22 ± 0.05	1.80	0.42 ± 0.08	7.4	4295 ± 1020
6240 ± 390	0.4	0.34 ± 0.16	0.80	0.57 ± 0.22	6.9	1515 ± 710
≈ 7755 ± 320	0.5 (estimated)	–	1.00	–	7.0	–

during the Holocene. Three Holocene earthquakes have been identified on the Oca fault, dated slightly prior to 7755 ± 320, 6240 ± 390 and 1945 ± 630 yr B.P. (Table 1).

The occurrence of the oldest of these three events is just an estimate based on sedimentary criteria (Table 1), as it can be observed in Fig. 4: the fault controls sedimentation of the lower part of the thickest sandy bed of the footwall block dated at 7755 ± 320 yr B.P.

As mentioned earlier, if sedimentation had not been conditioned by vertical movements on the fault, we could have believed that bending, which deforms the whole sequence in 0.9 m, and faulting, which vertically displaces the thickest silty-sand layer 0.4 m, might have happened simultaneously during a single earthquake, but the occurrence of at least two seismic events during deposition of the upper part of the sequence is necessary to explain the persistence of channels in the footwall and the difference in thickness of several sandy markers present in both blocks.

We consider that the penultimate earthquake conditioned the location of the channel in the footwall block. Therefore, occurrence of this earthquake is slightly prior to channel erosion and it can be fixed at 6240 ± 390 yr B.P. (Fig. 3, between HG-10 and HG-11 sample ages). This seismic event is associated to the 0.4-m vertical displacement of the thickest sandy marker and it is responsible for the gentle north tilting of the hanging-wall block. If the measured 30° slickenside is considered, the observed vertical displacement yields a 0.8-m coseismic displacement along the Oca fault plane which can generate an earthquake of magnitude (M_s) 6.9, after the relationship of Utsu and Seki (1954) (Table 1).

The latest earthquake, and by far the greatest, occurred between 2735 ± 160 (age of last correlatable marker between both blocks; HG-13 sample) and 1190 ± 125 (age of organic-soil base; sample HG-14). The coseismic vertical displacement, which has mainly been accommodated by bending, is 0.9 m. As for the penultimate earthquake, this value corresponds to a 1.8-m total displacement, potentially producing an earthquake of magnitude (M_s) 7.4. Recurrence of such events is as much as 4295 ± 1020 yr, the time elapsed between the two latest events (Table 1).

7. The Hato La Pica trench on the Ancón fault

At the selected trench site, the Ancón fault corresponds to a several kilometers long, north-facing scarplet. The trench site is located some 5 km north of the Maracaibo–Coro road and slightly west of the Cocuiza river, in Zulia State.

The following main observations were made at the trench site:

(a) The scarplet strikes east–west and it faces north. It is slightly smoothed and subdued by erosion (Fig. 5). Difference in height introduced by the Ancón fault between both blocks is 1.2 m.

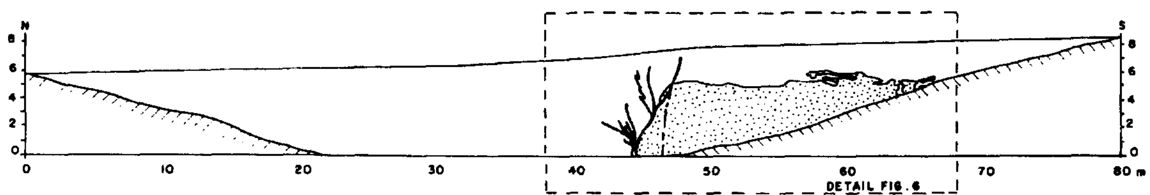

Fig. 5. Log of the Hato–La Pica trench across the Ancón fault.

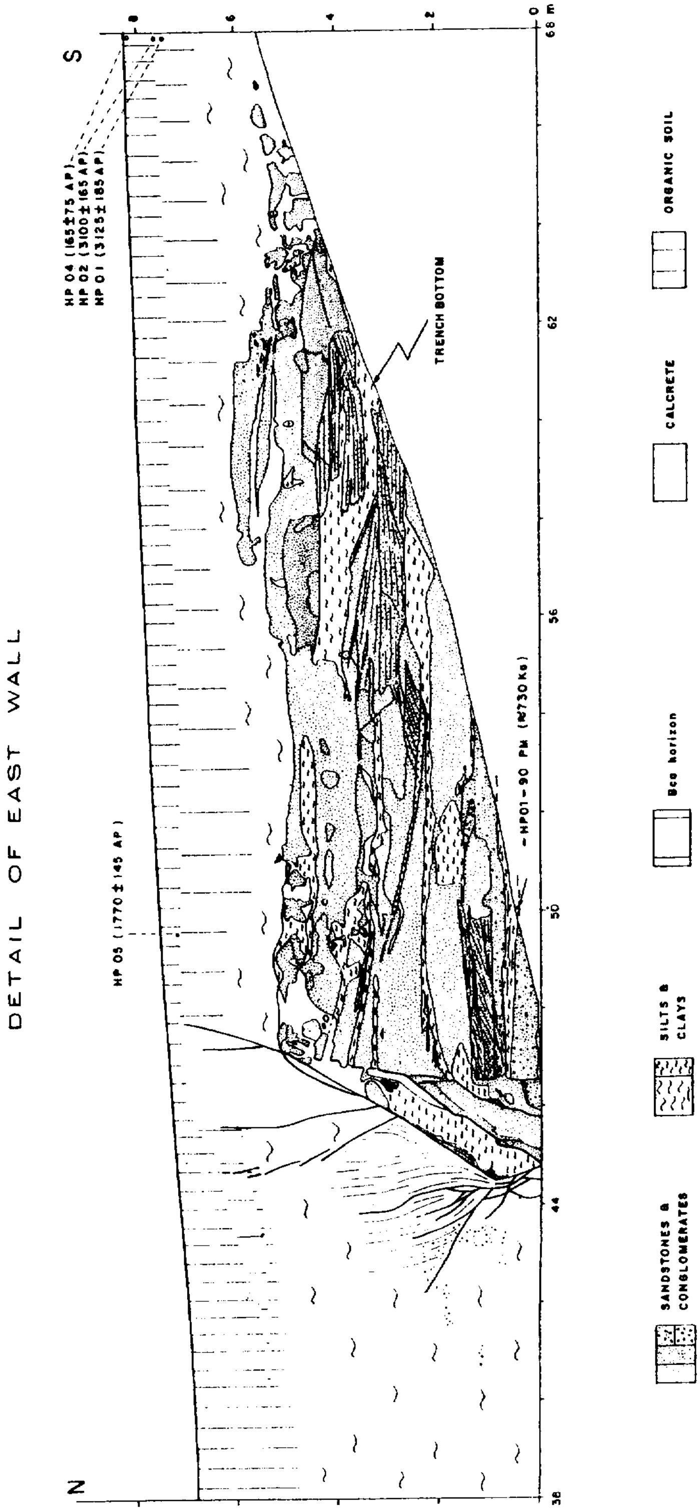

Fig. 6. Detail of the eastern wall of the Hato–La Pica trench.

(b) In trench walls, the scarp corresponds to a clearly visible fault zone. It stands out because of its white color, attributable to enrichment with carbonates by long-lasting water percolation along the fault plane. This assumption might be reinforced by the fact that the tallest trees of the site have grown along the fault trace, reflecting the presence of a densely fractured and highly permeable ground.

(c) The fault juxtaposes two completely different sedimentary sequences (Figs. 5 and 6): (1) the apparent downthrown block shows a very monotonous, brownish clayey sequence; and (2) the southern block is mainly constituted by a pebbly-to-sandy sequence bound by iron and manganese cement. This well-cemented unit is overlain by a 2-m-thick deposit equivalent to the one observed in the downthrown block.

(d) The organic soil developing on top of all is much thicker in the apparently downthrown block than in the upthrown (southern) block (Fig. 6).

(e) The age of the iron-bound sequence is about the Bruhnes–Matuyama paleomagnetic reversal ($\approx$ 730,000 years) as a sample collected from a clay bed belonging to that sequence, near the bottom of the trench, yielded such an age.

(f) The fault zone is up to 5 m wide and it is composed by a main fault plane, from which minor faults branch, presenting a wedge shape (Figs. 5 and 6).

(g) The main fault is characterized by the following: strike varies between N083 and N110°; dip is variable — the upper part of the fault plane dips north (76°N) whereas the lower part dips south (70°S); slickensides are perfectly horizontal (0°); consistent and coherent tectoglyphs (fault plane markers) point out a right-lateral movement; a 4-cm vertical throw is measured at the organic-soil base.

(h) The minor faults are reverse-dextral to sinistral-reverse and throws on them measured at the organic-soil base vary between 2 and 12 cm (Fig. 6).

The above-mentioned observations indicate that the fault is not of the simple type because the variable plane geometry (different dips on the plane) generates a fault-controlled wedge which helps to accommodate the apparent downthrow of the northern block (we must keep in mind that slickensides on the main plane are horizontal). The minor-fault movement splits such downthrow at the dip-change point, allowing a greater vertical movement far from the fault plane than next to its N-dipping part. Thus, this irregular geometry of the main fault explains why minor faults are mainly reverse.

8. Paleoseismic interpretation of the Hato–La Pica trench

Juxtaposition of such different sequences as those cropping out in each block within the trench indicates that deformation resulted from many recurrent earthquakes. However, recognition of the latest seismic event was possible since the organic-soil base has been deformed by the main fault plane in 4 cm (Fig. 6). Moreover, the same marker is also deformed by minor faults (Fig. 6). These ruptures seem not to cut the upper part of the soil. Therefore, occurrence of this earthquake may be fixed at 2467 $\pm$ 843 yr B.P., between ^{14}C samples VEN-90/HP-01 (3125 $\pm$ 185 yr B.P.) and VEN-90/HP-05 (1770 $\pm$ 145 yr B.P.) (Fig. 6). Nevertheless, trench information could not solve an apparent contradiction: movement along the fault is purely horizontal (as evidenced by slickensides) but a small vertical component is measured at the organic-soil base and a N-facing scarplet exists. So a three-boring campaign was carried out. These borings, joined to the trench, allowed to make a panel correlation. This correlation revealed the following facts (Fig. 7): the iron-bound sequence was found 15–16 m deeper in the apparent down-thrown block, which confirms the important cumulative deformation resulting from many recurrent earthquakes; the sedimentary sequence dips gently to the west ($\leq$ 1°W) along the fault strike, which agrees with the northwestward gentle slope of this coastal plains. Thus, the slightly oblique attitude of the sequence with respect to the fault explains how a pure horizontal movement along the Ancón fault can produce an apparent vertical displacement on the cut sequence markers and a north-facing fault scarp (Fig. 8).

Taking into account the previous facts (horizontal slickensides, $\leq$ 1°W dipping sequence and 4-cm apparent throw related to the latest earthquake), the total displacement responsible for that earthquake can be estimated at 2.3 m. After the empirical relationship of Utsu and Seki (1954), such a displacement may produce earthquakes of magnitude (M_s) 7.5.

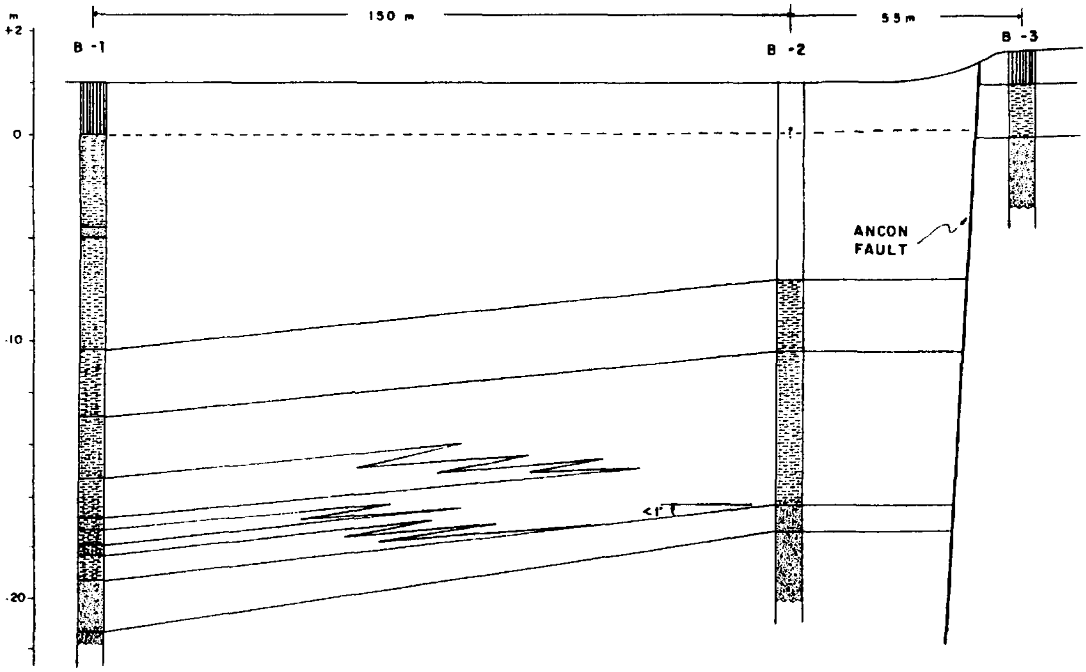

Fig. 7. Stratigraphic correlation of three borings located by the Ancón fault, next to the Hato–La Pica trench. The sandy unit at the boring bottoms corresponds to the sandstone–conglomerate unit observed in trench walls.

Besides, an average slip rate of the Ancón fault can be calculated if the following boring data are taken into account: 15.5–18.0 m of vertical throw measured at the top of the iron-bound sequence; top of this unit dips ≤ 1° W. Two additional considerations are required: age of this unit is about the

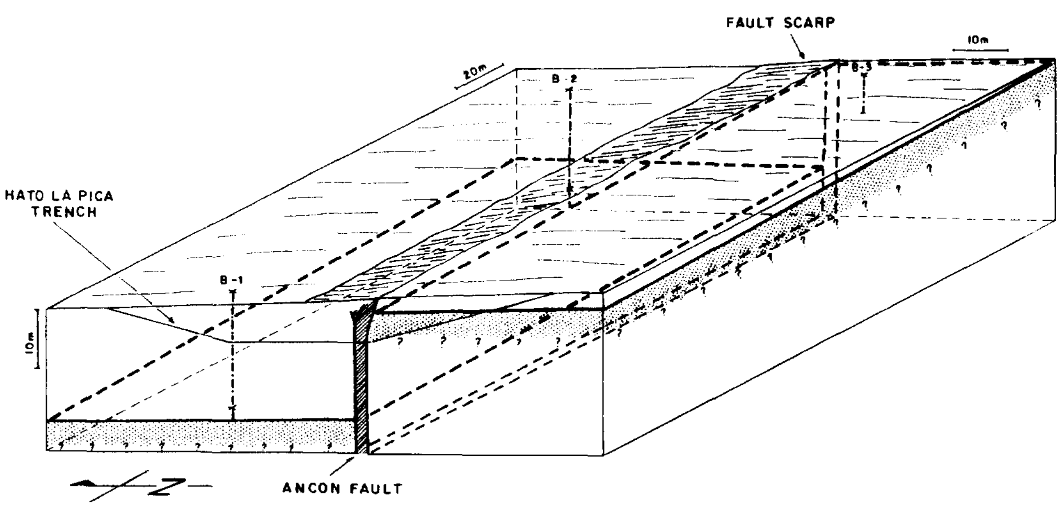

Fig. 8. Block diagram of the Hato–La Pica trench site showing the relationship between the sedimentary sequence and the Ancón fault plane. Note location of borings with respect to the trench and to the Ancón fault.

Bruhnes–Matuyama paleomagnetic reversal (≈ 730,000 years) and we assume movement along the Ancón fault has been constant since the Early Pleistocene. Then, displacement since the Early Pleistocene can be estimated at 960 ± 70 m and the average slip rate could be 1.32 ± 0.10 mm/yr.

To conclude, the probability of occurrence of a 7.5 earthquake on the Ancón fault is very high and close to a 100% because such earthquakes result from a 2.3 m total coseismic displacement which, at a slip rate of 1.32 ± 0.10 mm/yr, can be accumulated in 1752 ± 133 yr and the latest event on that fault happened between 1625 and 3310 yr B.P.

9. Latest events on the Oca and Ancón faults

By comparing the occurrence of the latest event on each fault (2467 ± 843 yr B.P. on the Ancón fault and 1945 ± 630 yr B.P. on the Oca fault), a certain contemporaneity between them arises since they overlap between 2575 and 1624 yr B.P. (some 900 years). Taking into account this possible contemporaneity, different scenarios can be proposed:

(a) Both faults have moved simultaneously. This is possible because the two faults seem to become a single fault at depth as suggested by seismic profiles interpreted by Audemard (1991) across segment B of the Oca–Ancón fault system;

(b) Movement on one fault has prompted movement on the other fault; or

(c) This contemporaneity is completely fortuitous and movements on both faults are totally independent in time as in space.However, information is inadequate to choose one alternative from the others.

On the contrary, it is amazing how similar the age determinations of the latest earthquake on the Oca fault made at two trenches [1920 ± 780 yr B.P. at Sinamaica and 1945 ± 630 yr B.P. (cf. Table 1) at Hato El Guayabal] are. Therefore, we could assume that both deformations are related to a single earthquake and connected by a 120 km long surface rupture distance between both trenches. After the empirical relationship of Slemmons (1977), such a rupture could be responsible for earthquakes of magnitude (M_s) 7.4, which is in perfect agreement with the magnitude calculated from the total displacement measured at the Hato–El Guayabal trench.

10. Overall slip rate of the Oca–Ancón fault system

The first slip-rate estimate of the Oca–Ancón fault system was proposed by Vasquez and Dickey (1972) who calculated it at 3 mm/yr based on the assumption that folding of the Falcón basin was produced by wrenching along the Oca–Ancón fault system. This figure might be correct or close to the real slip rate but the assumption is highly controversial as folding might be simply related to the regional tectonic regime and not to transpression along the Oca–Ancón fault. Later, Soulas et al. (1987) have calculated the slip rate of this system ranging between 2.5 and 4.0 mm/yr based on offsets of various geomorphic features of different Quaternary ages.

As we have described above, the Oca–Ancón fault system in its segment B, where trenching was carried out, is composed of two sub-parallel active faults: the Oca and Ancón faults. Therefore, the overall slip rate of this system can be estimated by summing up the individual slip rates of the Oca and Ancón faults estimated at each trench site. The Oca fault at the Hato–El Guayabal trench presents a slip rate that varies between 0.42 ± 0.08 and 0.57 ± 0.22 mm/yr (Table 1), whereas the slip rate of the Ancón fault is 1.32 ± 0.1 mm/yr. Thus, the overall slip rate of the system might be ranging between 1.56 and 2.21 mm/yr (≈ 1.88 ± 0.33 mm/yr). Nevertheless, it is worth mentioning how strongly dependent on the sequence dip is our slip rate estimate of the Ancón fault. For instance, instead of considering that the sequence dips ≈ 1°W as we previously did, if the dip is reduced to 0.8°W, then the new slip rate value increases up to 1.65 ± 0.15 mm/yr. This value is very similar to the one proposed by Soulas et al. (1987) based on an early Quaternary geomorphic feature (1.65 ± 0.35 mm/yr).

The great difference between the overall slip rate of this work based on trenches and that of Soulas et al. (1987) depends on the Oca fault slip rate estimates. Soulas et al. (1987) proposed that rate is between 1.0 and 2.0 mm/yr while trench evaluation constrains that value to be below 0.79 mm/yr and it should be more precisely about 0.56 ± 0.23 mm/yr. We consider that the value of Soulas et al. (1987) is overestimated because a slip rate estimate very similar to ours is obtained (0.42 ± 0.03 mm/yr) if other geomorphic data from the Dabajuro area indicated by those workers are taken into account.

In conclusion, it is reasonable to fix the overall slip rate of the Oca–Ancón fault system at 1.88 ± 0.33 mm/yr if the whole movement of the fault system in segment B occurs along the Oca and Ancón faults.

11. Conclusions

The following conclusions can be drawn from our trench studies across the Oca–Ancón fault system:

(a) The Oca and Ancón faults are both right-lateral and the Oca fault exhibits a reverse component. The Oca–Ancón fault system is transpressional along segment B and we believe that it behaves in the same way throughout the length of the E–W-striking segments.

(b) Three earthquakes have been identified on the Oca fault, dated slightly prior to 7755 ± 320, 6240 ± 390 and 1945 ± 630 yr B.P. Since the youngest deformation observed in the Hato–El Guayabal trench is so similar in age to that of the Sinamaica trench, we believe that the latest earthquake was produced by a 120 km long surface rupture, a length that is equivalent to the distance between these trenches. Such a rupture could be responsible for earthquakes of M_s 7.4, this value being in perfect accordance with the magnitude calculated empirically from the total displacement measured in the Hato–El Guayabal trench.

(c) One surface rupture event has occurred on the Ancón fault between 3125 ± 185 and 1770 ± 145 yr B.P. (2467 ± 843 yr B.P.).

(d) The Holocene slip rate of the fault system is about 1.88 ± 0.33 mm/yr. This slip rate is roughly partitioned into one quarter along the Oca fault and three quarters on the Ancón fault.

(e) Both the Oca and Ancón faults can generate a maximum earthquake of magnitude 7.4–7.5. The recurrence of such events on the Ancón fault is close to 1900 years, whereas it is more than twice as long on the Oca fault (4300 years).

Acknowledgements

I gratefully acknowledge MARAVEN S.A. for financing the trench excavations and age determinations. I also want to thank my FUNVISIS (Department of Earth Sciences) colleagues José Antonio Rodríguez, Carlos Chacín and Alfonso Adrianza for their helpful company during trench excavations and studies. My thanks to André Singer for the enlightening discussions. I am indebted to R. Russo and C. Vita-Finzi for their helpful and critical reviews of this paper.

References

Audemard, F.A., 1991. Actividad cuaternaria y caracterización sismogénica de las fallas de Lagarto y Río Seco. Afinamiento de las características sismogénicas del sistema de fallas de Oca–Ancón y Urumaco. Co. Rep., MARAVEN S.A., Caracas, 91 pp. (unpubl.).

Audemard, F.A., 1993. Néotectonique, sismotectonique et aléa sismique du nord-ouest du Vénézuéla (système de failles d'Oca–Ancón. Ph.D. Thesis, Montpellier II (U.S.T.L.), 369 pp.

Audemard, F.A. and Romero, G., 1993. The Churuguara area — Seismic evidence of contemporary activity of the Oca–Ancón system. Caribbean Conference on Natural Hazards: Volcanoes, Earthquakes, Windstorms, Floods. St. Augustine, Trinidad, pp. 21–32.

Audemard, F.A., Singer, A., Beltrán, C., Rodríguez, J.A., Lugo, M., Chacín, C., Adrianza, A., Mendoza, J. and Ramos, C., 1992. Actividad tectónica cuaternaria y características sismogénicas de los sistemas de falla de Oca–Ancón (tramo oriental), de la Península de Paraguaná y región de Coro y de la costa nororiental de Falcón. Co. Rep., Intevep S.A., Los Teques, 245 pp. (unpubl.).

Bellizzia, A., Rodríguez, D. and Graterol, M., 1972. Ofiolitas de Siquisique y Río Tocuyo y sus relaciones con la falla de Oca. VI Conf. Geol. Caribe, Margarita, Venezuela, pp. 182–183.

Cabrera de Molina, E., 1982. Geología petrolera de la cuenca de Falcón y su plataforma continental. EPC-10968 Co. Rep. MARAVEN S.A., Caracas, 34 pp. (unpubl.).

Cabrera de Molina, E., 1985. Evolución estructural de Falcón Central. M.Sc. Thesis, Esc. Geol. Min. Geof., Univ. Central de Venezuela, 59 pp.

Cisternas, A. and Gaulon, A., 1984. Síntesis sismotectónica del nordeste de Venezuela. Rev. Geofís., 40: 3–10.

Cluff, L. and Hansen, W., 1969. Seimicity and seismic geology of northwestern Venezuela. EPC-70480-I Co. Rep., MARAVEN S.A., Caracas (unpubl.).

Dewey, J., 1972. Seismicity and tectonics of western Venezuela. Bull. Seismol. Soc. Am., 62(6): 1711–1751.

Fichter, H.J., 1949. Comment on geological report CPMS-292. Recent faulting in the Buchivacoa–Miranda plains. EPC-852 Co. Rep. MARAVEN S.A., 6 pp. (unpubl.).

Gallardo, C., 1985. Esquisse sismotectonique de la region centro-occidentale du Vénézuéla et sa relation avec la géodynamique des Caraïbes. Ph.D. Thesis, Montpellier II (U.S.T.L.), 276 pp.

Graf, C., 1972. Relaciones entre tectonismo y sedimentación en el Holoceno del Noroeste de Venezuela. IV Congr. Geol. Venezolano, Bol. Geol., Publ. Esp., 5(2): 1125–1144.

Jaeckli, R. and Erdman, D., 1952. Geological compilation report Central and West Falcón. EPC-1272 Co. Rep., Shell, Venezuela (unpubl.).

Janssen, F., 1979. Structural style of Northwestern Venezuela. EPC-6270 Co. Rep., MARAVEN S.A., Caracas, 61 pp. (unpubl.).

Kafka, A. and Weidner, D., 1981. Earthquake focal mechanisms and tectonic processes along the Southern boundary of the Caribbean Plate. J. Geophys. Res., 86(B4): 2877–2888.

Kellogg, J. and Bonini, W., 1982. Subduction of the Caribbean Plate and basement uplifts in the overriding South-American Plate. Tectonics, 1(3): 251–276.

Malave, G., 1992. Inversión de ondas de volumen de algunos sismos importantes del noroccidente de Venezuela: relación con la tectónica regional. M.Sc. Thesis, Inst. Geofís., UNAM, México, 93 pp.

Malfait, B. and Dinkelman, M., 1972. Circum-Caribbean tectonic and igneous activity and the evolution of the Caribbean plate. Geol. Soc. Am. Bull., 83(2): 251–272.

Mendez, J. and Guevara, E., 1969. Geological compilation map of N.W. Venezuela, Guajira and Aruba (1:250,000). Co. Rep., MARAVEN S.A., Caracas (unpubl.).

Miller, J., 1960. Directrices tectónicas en la Sierra de Perijá y partes adyacentes de Venezuela y Colombia. III Congr. Geol. Venezolano, Caracas, 2: 685–718.

Morris, A.L., Taner, I., Meyerhoff, H.A. and Meyerhoff, A., 1990. Tectonic evolution of the Caribbean region; alternative hypothesis. In: The Geology of North America, H. Am. Geophys. Union, Boulder, CO, pp. 433–457.

Pindell, J., Cande, S., Pitman II, W., Rowlwy, D., Dewey, J., Labreque, J. and Haxby, W., 1988. A plate-kinematic framework for models of Caribbean evolution. Tectonophysics, 155: 121–138.

Schubert, C. and Krause, F., 1984. Moron fault zone, North-Central Venezuela borderland: Identification, definition and neotectonic character. Mar. Geophys. Res., 6: 257–273.

Schubert, C. and Sifontes, R., 1970. Boconó Fault, Venezuelan Andes: evidence of post glacial movement. Science, 170: 66–69.

Slemmons, D., 1977. State-of-the-art for assessing earthquake hazards in the United States: faults and earthquake magnitude. U.S. Army Eng. Waterways Exp. Stat., Soils Pavement Lab., Vicksburg, MS, Misc. Pap. S-73-1 6, 129 pp.

Soulas, J.-P., 1985. Neotectónica y tectónica activa en Venezuela y regiones vecinas. VI Congr. Geol. Venezolano, Caracas, 10: 6639–6656.

Soulas, J.-P., Giraldo, C., Bonnot, D. and Lugo, M., 1987. Actividad cuaternaria y características sismogénicas del sistema de fallas de Oca–Ancón y de las fallas de Lagarto, Urumaco, Río Seco y Pedregal. Afinamiento de las características sismogénicas de las fallas de Mene Grande y Valera. Co. Rep., MARAVEN S.A., Caracas, 69 pp. (unpubl.).

Stephan, J.-F., 1982. Evolution géodinamique du domaine Caraïbe, Andes et chaine Caraïbe sur la transversale de Barquisimeto (Vénézuéla). Ph.D. Thesis, Paris, 512 pp.

Stephan, J.-F., 1985. Andes et chaine caraibe sur la transversale de Barquisimeto (Vénézuéla). Evolution géodinamique. Symp. Géodynamique des Caraïbes, Paris, pp. 505–529.

Tschanz, C., Jimeno, A. and Cruz, B., 1969. Mapa geológico de reconocimiento de la Sierra Nevada de Santa Marta (1:200,000). Ingeominas, Bogotá.

Tschanz, C., Martín, R., Cruz, B., Mehnert, H. and Cebula, G., 1974. Geologic evolution of the Sierra Nevada de Santa Marta, northeastern Colombia. Geol. Soc. Am. Bull., 85: 273–284.

Vasquez, E. and Dickey, P., 1972. Major faulting in northwestern Venezuela and its relation to global tectonics. VI Conf. Geol. Caribe. Margarita, Venezuela, pp. 191–202.

Voorwijk, G., 1948. Recent faulting in the Buchivacoa–Miranda plains. EPC-852 Co. Rep., MARAVEN S.A., Caracas, 6 pp. (unpubl.).

Utsu, T. and Seki, A., 1954. A relation between the area of aftershock region and the energy of main shock. J. Seismol. Soc. Jpn., 7: 233–240 (in Japanese).